CHEMMEDCHEM

ChemPubSoc Europe

DOI: 10.1002/cmdc.201200058

Discovery of *N*-Arylalkyl-3-hydroxy-4-oxo-3,4-dihydroquinazolin-2-carboxamide Derivatives as HCV NS5B Polymerase Inhibitors

Ravindra Ramesh Deore,[a] Grace Shiahuy Chen,[a, b] Pei-Teh Chang,[a] Ting-Rong Chern,[a, c] Shin-Yu Lai,[a] Ming-Hsieh Chuang,[b] Jung-Hsin Lin,[a, c, d] Fan-Lu Kung,[a] Chien-Shu Chen,[a] Chun-Tang Chiou,[e] and Ji-Wang Chern*[a, f]

The metal ion chelating β-*N*-hydroxy-γ-ketocarboxamide pharmacophore was integrated into a quinazolinone scaffold, leading to *N*-arylalkyl-3-hydroxy-4-oxo-3,4-dihydroquinazolin-2-carboxamide derivatives as hepatitis C virus (HCV) NS5B polymerase inhibitors. Lead optimization led to the identification of *N*-phenylpropyl carboxamide **9k** (IC_{50} = 8.8 μM). Compound **9k** possesses selectivity toward HCV1b replicon Ava.5 cells (EC_{50} = 17.5 μM) over parent Huh-7 cells (CC_{50} = 187.5 μM). Compound **9k** effects a mixed mode of NS5B inhibition, with NTP-competitive displacement properties. The interaction between **9k** and NS5B is stabilized by the presence of magnesium ions. Docking studies showed that the binding orientation of **9k** occupies the central portions of both magnesium-mediated and NTP-ribose-response binding sites within the active site region of NS5B. As a result, 3-hydroxy-4-oxo-3,4-dihydroquinazolin-2-carboxamide derivatives are disclosed herein as novel, mainly active site inhibitors of HCV NS5B polymerase.

Introduction

Hepatitis C virus (HCV) is the major causative agent of chronic non-A, non-B hepatitis.[1] It is a hepatotropic single-stranded RNA virus that belongs to the genus *Hepacivirus*, family *Flaviviridae*. Chronic HCV infection leads progressively to major liver disorders such as cirrhosis, end-stage liver disease, and hepatocellular carcinoma.[2,3] Among six major genotypes that encompass nine different subtypes, HCV genotype 1 causes the majority of HCV infections.[4–6] Neither a vaccine nor an effective therapy against all HCV genotypes is available.[7] Current therapy involves a combination of ribavirin and PEGylated interferon (IFN)-α, which can enhance sustained virological response (SVR) rates to 54–56%.[8,9] However, this combination therapy does not show lasting improvement in 40–50% of HCV patients, and other disadvantages such as high cost and undesired side effects persist.[10]

The HCV NS5B polymerase is not expressed in host cells, and it is therefore considered as a potential target for HCV therapeutics. HCV NS5B polymerase is an RNA-dependent RNA polymerase that catalyzes the synthesis of both negative-strand copies of the incoming viral RNA and positive-strand progeny RNA genomes.[11] NS5B polymerase has a tertiary structure with three constitutive peptide domains known as the palm, fingers, and thumb.[12] Two magnesium ions, coordinated in the palm domain, facilitate the catalytic activity of HCV NS5B. A number of HCV NS5B polymerase inhibitors with structurally diverse scaffolds have been reported,[13] and inhibitors such as ANA598, BMS791325, Filibuvir, GS9190, PSI7977, RG7128, VX222, and VX759 have been advanced to phase II clinical trials.[14]

Most non-nucleoside NS5B polymerase inhibitors have been characterized as allosteric inhibitors and demonstrate potent inhibitory activity in cell-based assays. Although allosteric inhibitors provide favorable pharmacokinetic profiles, the emergence of resistant mutant viral strains limits their progress in the treatment of patients with chronic HCV infections.[15] However, the active site of NS5B polymerase still represents a potentially viable target. Active site residues Asp318, Asp319, and Asp220 are important for NS5B catalytic activity.[16] The active site forms complexes with two Mg^{2+} ions and coordi-

[a] *Dr. R. R. Deore,[+] Prof. G. S. Chen,[+] Dr. P.-T. Chang,[+] T.-R. Chern, Dr. S.-Y. Lai, Prof. J.-H. Lin, Prof. F.-L. Kung, Prof. C.-S. Chen, Prof. J.-W. Chern*
School of Pharmacy, National Taiwan University, Taipei 10051 (Taiwan ROC)
E-mail: jwchern@ntu.edu.tw

[b] *Prof. G. S. Chen,[+] M.-H. Chuang*
Department of Applied Chemistry
Providence University, Taichung 43301 (Taiwan ROC)

[c] *T.-R. Chern, Prof. J.-H. Lin*
Division of Mechanics, Research Center for Applied Sciences
Academia Sinica, Taipei 11529 (Taiwan ROC)

[d] *Prof. J.-H. Lin*
Institute of Biomedical Sciences
Academia Sinica, Taipei 11529 (Taiwan ROC)

[e] *Dr. C.-T. Chiou*
Division of Herbal Drugs and Natural Products
National Research Institute of Chinese Medicine, Taipei 11221 (Taiwan ROC)

[f] *Prof. J.-W. Chern*
Department of Life Science
National Taiwan University, Taipei 10617 (Taiwan ROC)

[+] *These authors contributed equally to this work.*

Supporting information for this article is available on the WWW under http://dx.doi.org/10.1002/cmdc.201200058.

nates with the β- and γ-phosphate groups of incoming ribonucleotide triphosphate (NTP) substrates to activate the 3′-hydroxy group of the primer strand toward nucleophilic attack by the α-phosphate.[17] Until now, only a few non-nucleoside NS5B active site inhibitors have been reported. Most of these are involved in divalent metal ion chelation and act as pyrophosphate mimics. HCV NS5B active site inhibitors such as α,γ-diketo acid (DKA) **1**,[18] monoethyl ester of meconic acid **2**,[19] dihydroxypyrimidine carboxylic acid **3**,[20] and isothiazole **4**[21] are divalent metal ion chelators (Figure 1). The HIV integrase inhibitors hydroxypyrimidinone **5**[22] (Raltegravir) and bicyclic pyrimidinone **6**[23] are also divalent metal ion chelators.

As part of our studies on anti-HCV agents,[24] 2-hydroxy-1-oxo-4-phenyl-1,2-dihydroisoquinolin-3-carboxylic acid (**7a**) was identified as an HCV NS5B inhibitor with moderate antiviral activity ($EC_{50} = 15.7$ μM) and good selectivity in HCV genotype 1b replicon Ava.5 cells.[25] However, 4-unsubstituted 2-hydroxy-1-oxo-1,2-dihydroisoquinolin-3-carboxylic acid (**7b**) is inactive toward HCV NS5B polymerase. In view of bicyclic pyrimidinone **6**[23] (an HIV integrase inhibitor) and *N*-hydroxypyridinone **8**[26] (an anthrax lethal factor inhibitor) as metal ion chelators, we anticipated that integration of the β-*N*-hydroxy-γ-ketocarboxamide pharmacophore into a bicyclic system would result in coordination with the magnesium ions. Thus, derivatization of carboxylic acid **7b** into *N*-benzyl carboxamide and scaffold hopping of isoquinoline to quinazoline led to quinazolinone derivatives **9** (Figure 2), which would serve as active site inhibitors of NS5B polymerase. Herein we report the synthesis and structure–activity relationship (SAR) of 3-hydroxy-4-oxo-3,4-dihydroquinazolin-2-carboxamide derivatives **9** as HCV NS5B polymerase inhibitors.

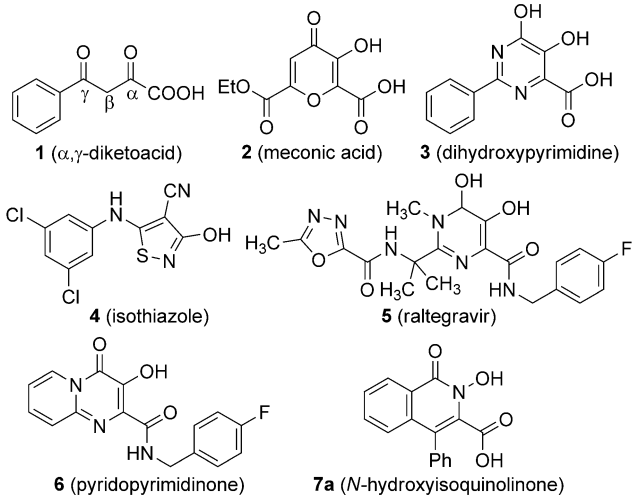

Figure 1. Divalent metal ion chelators as enzyme inhibitors.

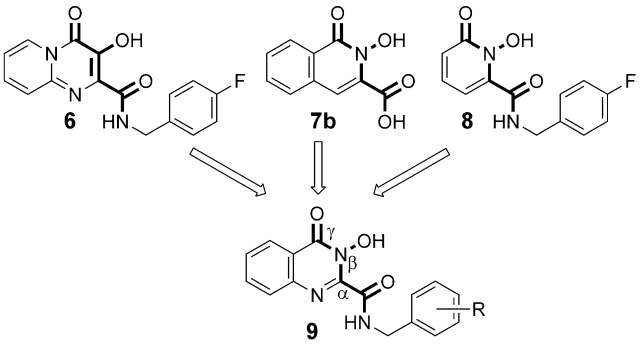

Figure 2. The design of β-*N*-hydroxy-γ-ketocarboxamide inbuilt quinazolinones **9** as pyrophosphate mimics for NS5B polymerase inhibitors.

Results and Discussion

Chemistry

Treatment of isatoic anhydride (**10**) with *O*-benzylhydroxyamine in the presence of triethylamine afforded 2-amino-*N*-benzyloxybenzamide **11** (Scheme 1). Compound **11** reacted with diethyl oxalate in the presence of catalytic amounts of *para*-toluenesulfonic acid, leading to ethyl *N*-benzyloxy-4-oxo-3,4-dihydroquinazolin-2-carboxylate (**12**), which underwent catalytic debenzylation over hydrogen in the presence of Pd/C to give β-*N*-hydroxy-γ-ketocarboxylate **13**. The ethyl carboxylate **13** was then treated with various amines to afford target compounds **9a**–**e** and **9g**–**k**. Alternatively, *O*-benzyl compound **12** could be derivatized to carboxamides **14a**–**d**, which were then debenzylated over hydrogen to give *N*-hydroxy derivatives **9**. In addition, nitro compound **9d** was reduced to its amino analogue **9f** by catalytic hydrogenation.

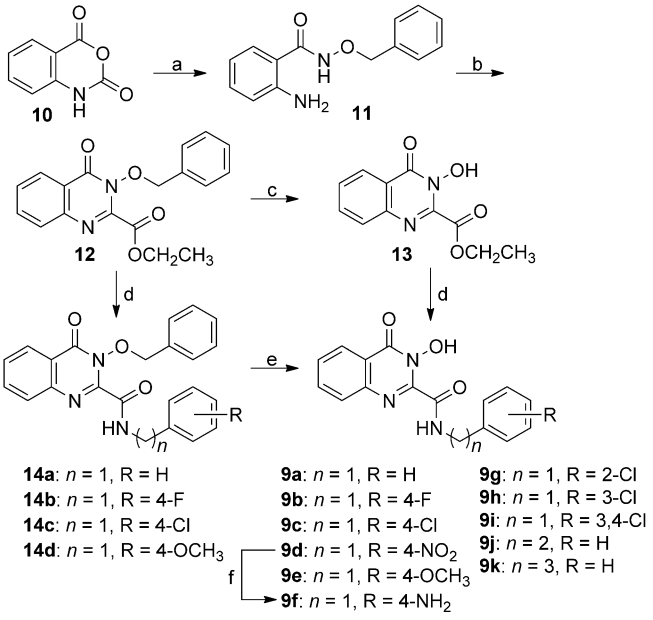

Scheme 1. *Reagents and conditions:* a) $PhCH_2ONH_2$·HCl, Et_3N, THF, reflux, 6 h; b) diethyl oxalate, *p*-TSA (cat.), reflux, 18 h; c) H_2, Pd/C (10%), EtOAc, RT, 30 min; d) arylalkylamines, EtOH, RT or reflux, 14–96 h; e) H_2, Pd/C (10%), EtOAc/MeOH (1:1), RT, 1 h; f) H_2, Pd/C (10%), EtOH, RT, 2 h.

Biological evaluation

HCV NS5B polymerase inhibitory activity

HCV NS5B polymerase activity was measured by the release of inorganic pyrophosphate (PPi), a nonradioactive assay for RNA-

dependent RNA polymerase activity.[27] Carboxamides **9** were evaluated for their inhibitory activity toward HCV NS5B polymerase by PPi inhibition assay, and the results are listed in Table 1. The reference compound DKA **1** showed moderate inhibitory activity, with an IC_{50} value of 20 μM. Compound **9a** possesses NS5B inhibitory activity (IC_{50} = 28 μM) similar to that of DKA **1**. The substituent effect on the *N*-benzyl group was examined. Derivatives with *N*-(4-fluorobenzyl) (**9b**), *N*-(4-chlorobenzyl) (**9c**), and *N*-(4-nitrobenzyl) (**9d**) groups lost inhibitory activity, with IC_{50} values of 45 μM or higher. *N*-(4-Methoxybenzyl) derivative **9e** showed a twofold enhancement in NS5B inhibitory activity (IC_{50} = 14 μM) relative to the parent compound **9a**, and *N*-(4-aminobenzyl) derivative **9f** was found to be roughly equipotent (IC_{50} = 30 μM) with **9a**. Whereas *N*-(4-chlorobenzyl)carboxamide **9c** is inactive toward the polymerase, *N*-(2-chlorobenzyl) (**9g**) and *N*-(3-chlorobenzyl) (**9h**) carboxamides possess inhibitory activity, with IC_{50} values of 33 and 26 μM, respectively. The *N*-(3,4-dichlorobenzyl) derivative **9i** is also active (IC_{50} = 28 μM). Thus, a chloro substituent at the *ortho* or *meta* positions of the *N*-benzyl group is tolerated, but not at the *para* position.

Table 1. Inhibitory activities against HCV NS5B polymerase and cytotoxicity toward parental Huh-7 cells and HCV replicon Ava.5/Huh-7 cells.

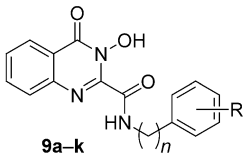

9a–k

Compd	R	*n*	IC_{50} [μM][a,b]	CC_{50} [μM][b]	EC_{50} [μM][b]	SI[c]
9a	H	1	28.2 ± 4.4	> 250	59.4 ± 8.1	> 4.2
9b	4-F	1	> 50.0	194.1 ± 16.5	54.4 ± 1.9	3.6
9c	4-Cl	1	44.5 ± 6.5	215.7 ± 24.9	76.3 ± 8.8	2.8
9d	4-NO_2	1	> 50.0	> 250	50.8 ± 2.9	> 4.9
9e	4-OCH_3	1	13.9 ± 2.9	175.0 ± 8.3	32.9 ± 5.2	5.4
9f	4-NH_2	1	29.9 ± 3.2	> 250	21.4 ± 3.7	> 11.9
9g	2-Cl	1	32.8 ± 3.3	224.8 ± 10.7	36.3 ± 8.7	6.2
9h	3-Cl	1	25.6 ± 2.7	> 250	29.6 ± 1.7	> 8.5
9i	3,4-diCl	1	28.1 ± 1.4	202.1 ± 23.3	33.8 ± 5.3	6.0
9j	H	2	46.1 ± 6.3	> 250	28.7 ± 5.4	> 8.7
9k	H	3	8.8 ± 1.6	187.5 ± 14.6	17.5 ± 2.5	10.7
1	–	–	19.9 ± 0.3	186.8 ± 19.1	127.6 ± 5.1	1.5

[a] NS5B inhibitory activity based on PPi generation. [b] IC_{50} (concentration required for 50% inhibition of NS5B activity), CC_{50} (cytotoxicity against Huh-7 cells), and EC_{50} (cytotoxicity against Ava.5, HCV replicon cells) values represent the mean ± SD of three independent experiments, each carried out in triplicate. [c] Selectivity index: CC_{50}/EC_{50}.

In addition, the linker chain of the *N*-arylalkyl carboxamide was extended. Compound **9j**, with an ethylene linker, showed decreased inhibitory activity (IC_{50} = 46 μM). Upon increasing the chain length to propylene, compound **9k** turned out to be the most potent inhibitor (IC_{50} = 9 μM) in this series of 3-hydroxy-4-oxoquinazolin-2-carboxamides.

Anti-HCV activities

Compounds **9a–k** and DKA **1** were found to be non-cytotoxic to the parental Huh-7 cell line (CC_{50} > 175 μM, Table 1). DKA **1** is not cytotoxic to HCV1b replicon Ava.5 cells (EC_{50} = 128 μM) despite its inhibitory activity toward NS5B polymerase (IC_{50} = 20 μM, Table 1). Compounds **9a–d** showed very weak cytotoxicity (EC_{50} > 50 μM) toward Ava.5 cells. Compounds **9e–k** exhibited better antiviral activity, with EC_{50} values ranging from 17 to 36 μM toward the Ava.5 cell line. The most potent inhibitor **9k** also demonstrated the highest antiviral activity (EC_{50} = 17 μM). As a result, compound **9k** possesses significant selectivity (SI > 10.7, Table 1) for HCV replicon Ava.5 cells. The trend in anti-HCV activity of compounds **9a–k** toward Ava.5/Huh-7 cells was observed microscopically through decreased cell number and cell swelling (Figure 3). The antiviral effect was also investigated at the HCV RNA level in HCV replicon Ava.5

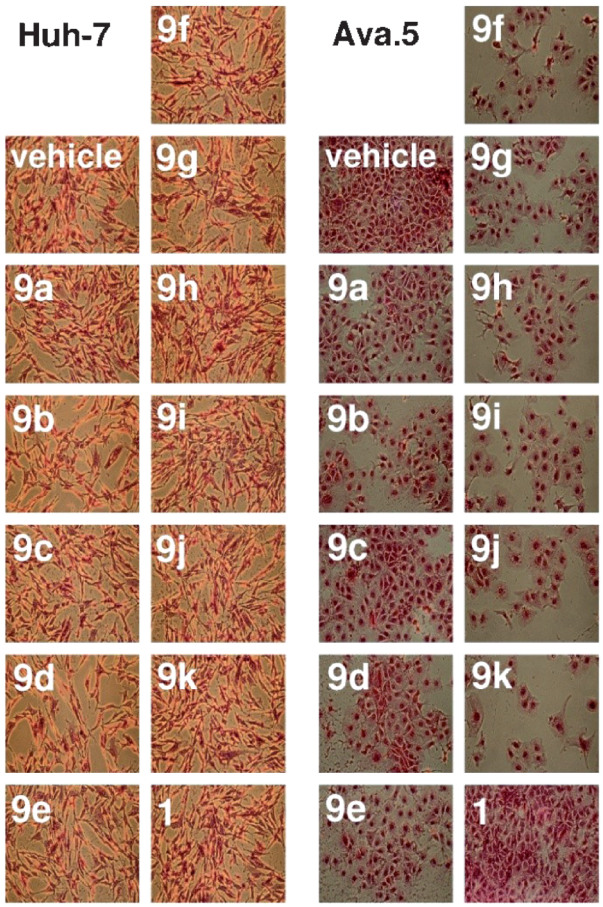

Figure 3. The effects on Huh-7 and Ava.5 cells. Microscopic morphologies (20×) of Huh-7 (right side) and Ava.5 (left side) cells after treatment with the indicated compounds followed by Giemsa staining. Images are from a representative experiment; at least three independent experiments with similar results were performed.

cells. Compound **9k** effectively decreased the RNA levels in HCV replicons at concentrations of 10 μM and above (Figure 4). In agreement with the results of cytotoxicity assessments with Ava.5 cells, DKA **1** showed no effect on RNA levels.

Inhibition mode on NS5B polymerase

The inhibitory profile of HCV NS5B polymerase activity was determined by using a PPi-based NS5B activity assay in the presence of NTPs and **9k**. As shown in Figure 5a, b, dose–response curves at the non-saturated NTP phase indicate that a substantial increase in NTP concentration affects the inhibitory activity of **9k** toward NS5B. The competitive and uncompetitive inhibition constants ($k_{ic}=0.64$ and $k_{iu}=3.94$, respectively) of **9k** were estimated according to the Lineweaver–Burk plots (Figure 5c, d), indicating that **9k** most likely acts as a competitive inhibitor ($k_{ic}<k_{iu}$). The kinetics of competitive inhibition was further examined by varying the concentration of **9k** in the presence of a fixed concentration of fluorescein-labeled GTP. Not only does compound **9k** effectively compete with GTP binding at NS5B, it displaces NTP binding as well (Figure 6). The effect of **9k** on NS5B might result in a decreased association between NS5B and NTP, from the NTP-free state of NS5B and the rate of NTP hydrolysis in the NTP-bound state of NS5B.

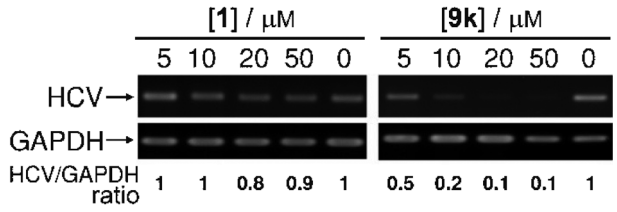

Figure 4. Effect of **9k** on HCV RNA levels in HCV replicon Ava.5 cells. A fully confluent monolayer of Ava.5 cells in a 10-cm Petri dish were treated with compounds **1** or **9k** at various concentrations for 24 h. After incubation, total RNA was extracted, and HCV or GAPDH mRNA levels were determined by semi-quantitative RT-PCR. The HCV/GAPDH ratio represents intensity relative to control (vehicle). Images were taken from a representative experiment; data represent the mean of three independent experiments, each performed in triplicate.

Binding affinity of 9k for NS5B polymerase

A quartz crystal microbalance (QCM) system was used to monitor the specific interaction between **9k** and NS5B. Compound **9k** has no adsorptions with a control and reference-protein-modified sensor (data not shown). Importantly, compound **9k** showed specific adsorption behavior with concentration-dependent frequency shifts (from 5 to 15 Hz) on the NS5B-coated sensor (Supporting Information). The extensive concentration range used allowed determination of the dissociation constant (K_d) of **9k** toward the NS5B binding site (Figure 7a). The K_d value (22 μM) was calculated from the double-reciprocal plot (Figure 7b). Although this result does not allow a determination as to whether **9k** binds NS5B solely at the active site, or at an allosteric site functionally coupled to the active site, this finding does provide compelling evidence that **9k** interacts with

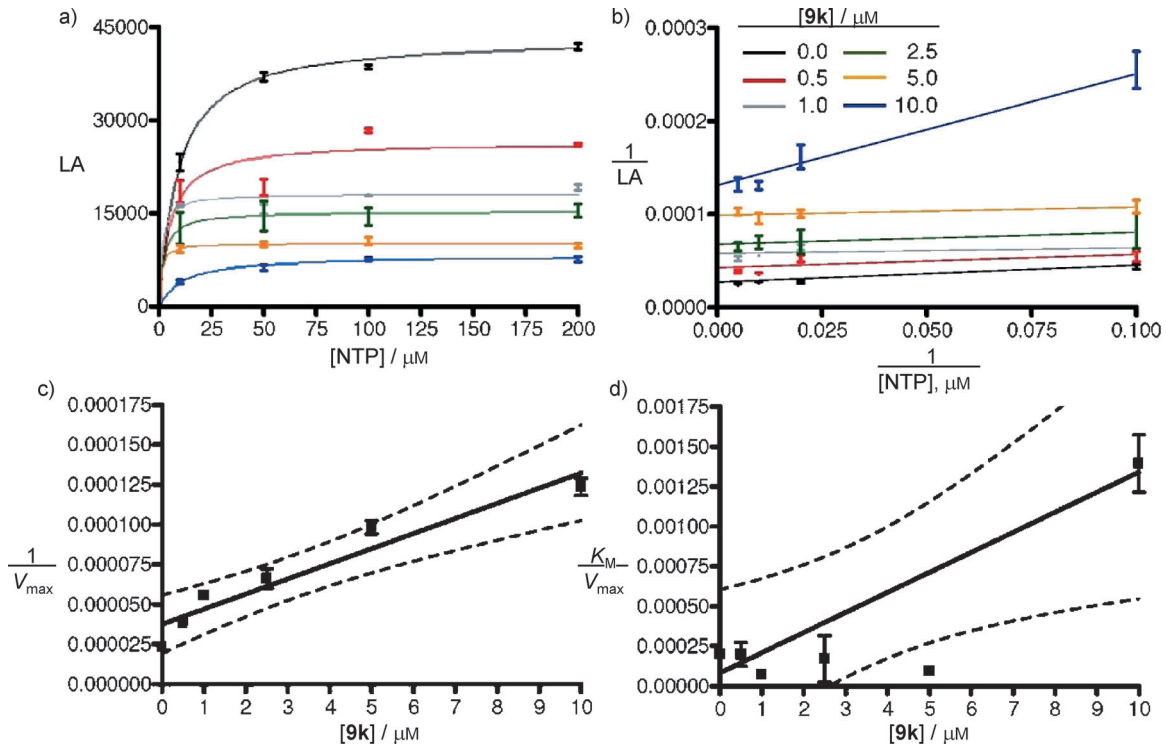

Figure 5. Model of inhibition and inhibition constants for compound **9k** toward NS5B polymerase kinetics. a) Michaelis–Menten and b) Lineweaver–Burk plots depict the effect of **9k** at concentrations of 0, 0.5, 1.0, 2.5, 5.0, and 10 μM on NS5B activity (LA: luminescence activity). Secondary plots were constructed and used to calculate the c) uncompetitive and d) competitive inhibition constants for **9k** on NS5B according to nonlinear regression analysis; data represent the mean ± SD from at least three independent experiments.

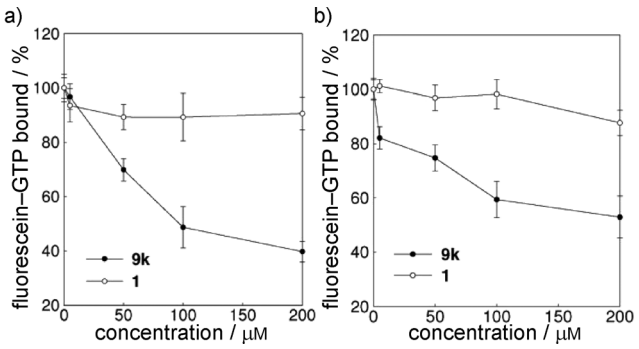

Figure 6. Competition and displacement of fluorescein-labeled GTP from NS5B polymerase. a) The binding of fluorescein-labeled GTP on NS5B was monitored simultaneously in the presence of **9k** (●) or **1** (○) at various concentrations. b) The preformed fluorescein-labeled NTP–NS5B complex was incubated with **9k** (●) or **1** (○) at various concentrations. Unbound fluorescein-labeled NTP was removed, and the fluorescence intensity of NS5B-bound NTP was measured; fluorescence from the group without NS5B inhibitors was taken as 100%, and fluorescence from the group without fluorescein–GTP was taken as 0%. Data represent the mean ±SD from three independent experiments, each performed in triplicate.

the NS5B active site. Both the level and rate of total binding at NS5B in the presence of biotin-11-GTP (M_r = 914 Da) and **9k** (M_r = 323 Da) were lower than those in the presence of biotin-11-GTP alone (Figure 7c). The changes in both early association rate (twofold increase in slope during the first 50 s) and kinetic level (24% frequency increase at 200 s) for NS5B binding were dominated by **9k**, suggesting that the binding of **9k** at NS5B likely results in the occlusion or interference with the association of NTP with the NS5B active site region. Furthermore, the interaction between **9k** and NS5B is significantly affected by the presence of magnesium ions (Figure 7d). The magnesium-dependent binding of **9k** and this compound's ability to impede the association of NTP with NS5B further confirm that **9k** binds NS5B principally at the active site region.

Molecular modeling

A docking study was performed to explore the interactions between **9k** and NS5B polymerase. As shown in Figure 8, compound **9k** interacts with one magnesium ion present in the active site (Asp 318–Asp 319–Asp 220), which is indispensable to the polymerase-catalyzed nucleotidyl transfer reaction. Superimposition of **9k** and crystallographic UTP (Figure 8a) shows that **9k** chelates the same magnesium ion that is chelated by the β- and γ-phosphate groups of UTP. The binding pose is consistent with one previously reported.[28] Unlike the hydrogen bonding interactions established between the pyrimidine nucleobase of UTP and polar residues of NS5B, the hydrophobic phenylpropylene group of **9k** is inserted into a hydrophobic region in the enzyme consisting of Leu 159 and Val 52. There are several residues involved in the interaction (Figure 8b,c). The amide group of **9k** forms a hydrogen bond with the backbone group of Asp 225, the same residue that is

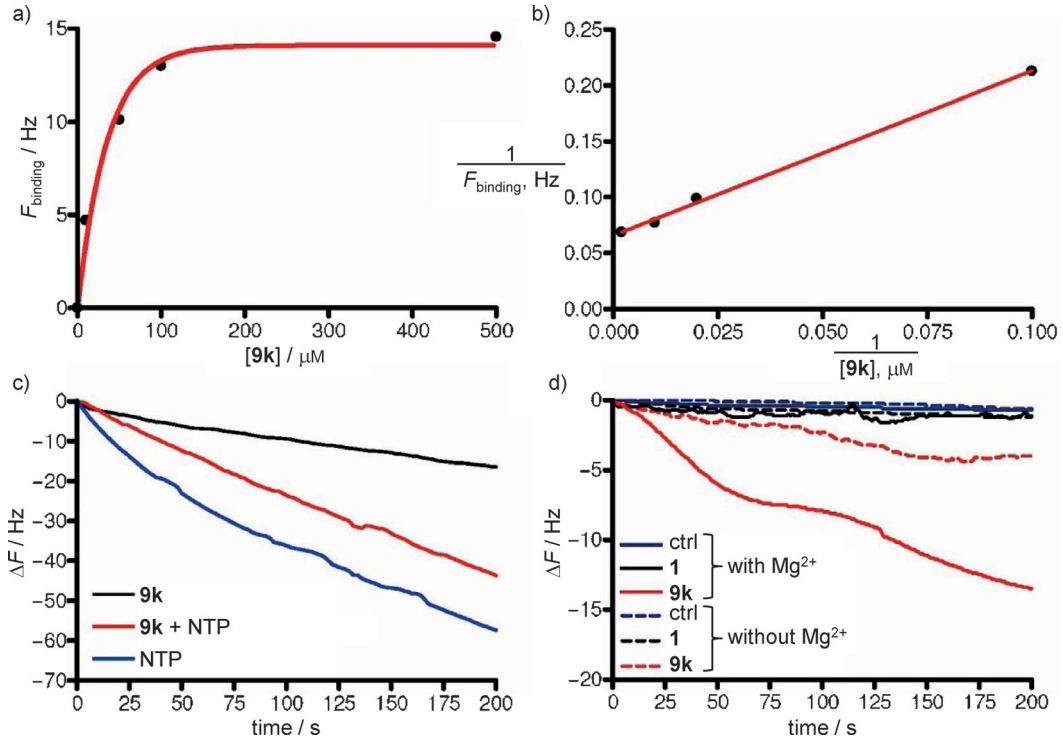

Figure 7. The binding of compound **9k** to NS5B as measured by QCM coated with NS5B (5 μg mL^{-1}). The a) dose–response binding curve and subsequent b) linear reciprocal plot for **9k** binding with NS5B are plotted according to the frequency changes at 200 s. c) Biotin–NTP (blue, 200 μM) and **9k** (black, 200 μM) were added individually or simultaneously (red, 200 μM each) to identify the total NS5B binding changes during the combination of NTP and **9k**. Experiments shown in panels a)–c) were carried out in the presence of magnesium. d) Compounds **9k** (red) and **1** (black) were added to NS5B at conditions with (solid lines) or without (dashed lines) magnesium; vehicle controls (ctrl) are shown in blue. Experiments were carried out in triplicate and gave similar resulting frequency shifts.

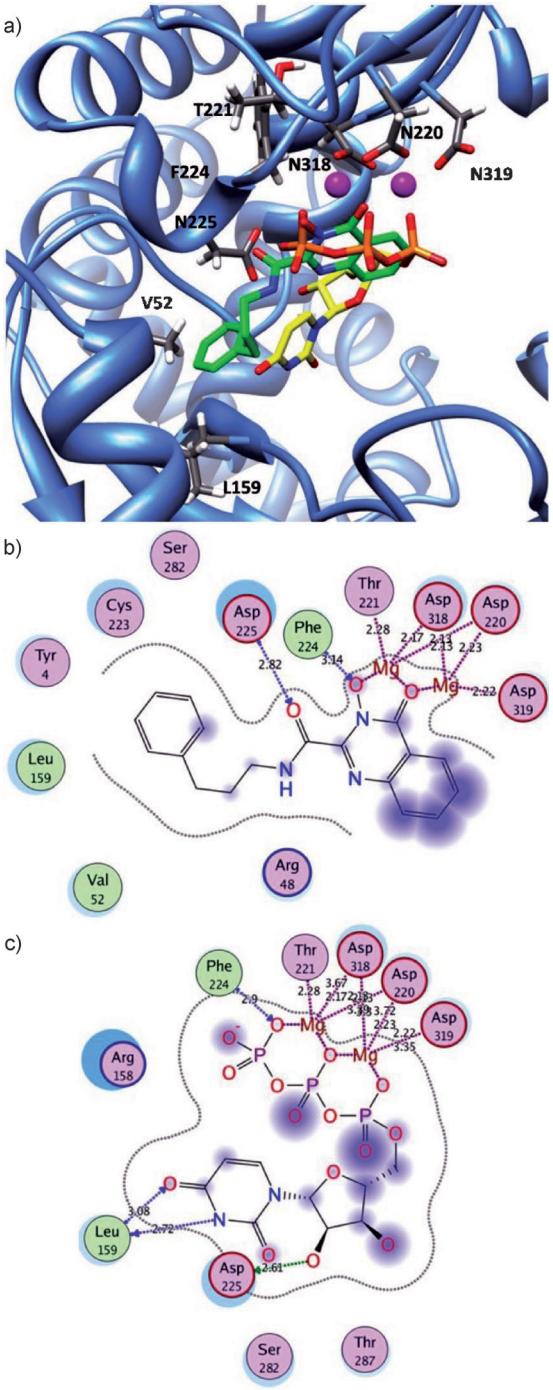

Figure 8. Docking model of **9k** into the NS5B active site. a) The superimposed predicted binding pose of compound **9k** (green) and the crystallographically determined orientation of NTP (yellow) in the catalytic site of NS5B. The two Mg^{2+} ions are indicated as magenta spheres, oxygen atoms are shown in red, nitrogen in blue, and phosphorus in orange. Interactions of b) compound **9k** and c) UTP with NS5B active site residues. Residues within 4.5 Å of **9k** are presented in the 2D interaction diagram. Purple circles on the ligand represent the intensity of solvent exposure: the larger the circle, the greater the exposure of ligand to the solvent. Green, blue, and magenta dashed lines represent side chain hydrogen bonds, backbone hydrogen bonds, and metal chelation interactions, respectively. The two oxygen atoms of compound **9k** are chelated with magnesium ions. The bond lengths of chelating interactions between molecular atoms and metal ions range between 2.1 and 3.7 Å. Residues in green circles are hydrophobic; residues circled in red and blue represent acidic and basic properties, respectively.

hydrogen bonded to the 2′-hydroxy group of UTP. The 3-hydroxy group of **9k** is also hydrogen bonded to Phe 224, which interacts with the triphosphate group of NTP substrates. The phenylpropylene group of **9k** forms hydrophobic interactions with Leu 159, which interacts with the pyrimidine base of UTP. We therefore reasoned that these hydrogen bonding and hydrophobic interactions, together with magnesium chelation, contribute to the overall binding of **9k** to NS5B.

Physicochemical studies

N-Arylalkyl-3-hydroxy-4-oxoquinazolin-2-carboxamides **9** were designed as divalent metal ion chelating pyrophosphate mimics, like the DKA prototype. Accordingly, the interaction of compound **9k** with magnesium ions was examined by ^{1}H NMR spectroscopy (Table 2 and Supporting Information). Incubation of compound **9k** (0.01 M in [D_6]DMSO) with $MgCl_2{\cdot}6H_2O$ (2 equiv) had little or no effect on the ^{1}H NMR spectrum of **9k**.

Table 2. Change in chemical shift values of **9k** upon incubation with $MgCl_2{\cdot}6H_2O$, H_2O, $Mg(OAc)_2{\cdot}4H_2O$, and NaOAc.

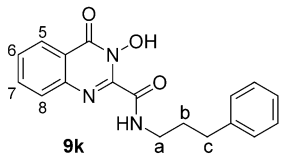

9k

Proton	Δδ [ppm]			
	$MgCl_2{\cdot}6H_2O$	H_2O	$Mg(OAc)_2{\cdot}4H_2O$	NaOAc
H-5	0.00	−0.02	−0.05	−0.26
H-6	0.00	−0.01	−0.01	−0.15
H-7	0.00	0.00	−0.04	−0.20
H-8	−0.01	−0.02	+0.12	−0.08
NH	+0.03	+0.02	+0.74	+0.46
H-a	0.00	−0.02	+0.06	+0.02
H-b	−0.01	−0.02	−0.01	+0.01
H-c	−0.01	−0.03	+0.06	+0.02

To confirm the effect of hydrate in $MgCl_2{\cdot}6H_2O$, the ^{1}H NMR spectrum of **9k** in the presence of 10% water was recorded with negligible modifications.[25,29] Thus, compound **9k** did not chelate the magnesium ion under neutral conditions. However, the OH peak ($\delta = 12.05$ ppm) disappeared, and the NH peak ($\delta = 8.95$ ppm) shifted downfield by 0.74 ppm with loss of resolution upon addition of $Mg(OAc)_2{\cdot}4H_2O$ (2 equiv) to **9k** (0.01 M in [D_6]DMSO). Propylene protons were consequently shifted downfield. The ^{1}H NMR spectrum of **9k** (0.01 M in [D_6]DMSO) in the presence of sodium acetate resulted in a downfield shift of the NH signal by $\delta = 0.46$ ppm and upfield shifts of all protons on quinazolinone ring. On the basis of these results, it was proposed that the weak base acetate ion causes partial deprotonation of **9k**, which then chelates magnesium ions upon addition of magnesium acetate.

Conclusions

N-Arylalkyl-3-hydroxy-4-oxo-3,4-dihydroquinazolin-2-carboxamide derivatives **9a**, **9e–i**, and **9k** were identified as HCV NS5B polymerase inhibitors. Compound **9k** was discovered as a mixed-type competitive inhibitor against NS5B polymerase, with an IC_{50} value of 8.77 μM; it possesses selective cytotoxicity, with an EC_{50} value of 17.5 μM toward HCV1b replicon Ava.5 cells. Competitive displacement and docking studies illustrated that the 3-hydroxy-4-oxo-2-carboxamide moiety of **9k** might interact with two magnesium ions like pyrophosphate mimics in the NS5B polymerase active site. As a result, integration of the β-*N*-hydroxy-γ-ketocarboxamide pharmacophore into a bicyclic system such as that represented by 3-hydroxy-4-oxo-3,4-dihydroquinazolin-2-carboxamide derivatives could give rise to a series of HCV NS5B polymerase inhibitors.

Experimental Section

Chemistry

All chemical reagents and solvents were obtained from commercial sources (Merck, Mallinckrodt, Acros, Lancaster, Aldrich, and TCI) and were used without further purification. Reaction progress was monitored by thin-layer chromatography (TLC) analysis on silica gel 60 F_{254} plates (Merck), visualized by UV light. Chromatographic purification was carried out on silica gel columns (Silica gel Si 60, 40–63 μm, Merck). Melting points were determined with a Mel-Temp melting point apparatus, and are uncorrected. NMR spectra were recorded on AMX-400 (Bruker) and DPX-200 (Bruker) spectrometers. MS (ESI) spectra were recorded on a Finnigan TSQ 7000 with ESI mode negative ion trap detector. HRMS data were obtained with ESI mode positive ion trap. Elemental analyses were recorded on Thermo Flash 2000 (for N, C, S, H). Purity (>95%) determinations were performed by HPLC (column: Merck LiChrospher 100 RP-18e; pump A type: L-7100; injection volume: 20 μL (100 μg mL^{-1} for each compound); detector: Hitachi UV/Vis L-7420, λ 254 nM).

2-Amino-*N*-benzyloxybenzamide (11): To a mixture of isatoic anhydride (**10**) (10 g, 61.3 mmol) and *O*-benzylhydroxyamine hydrochloride (11.74 g, 73.6 mmol) in anhydrous THF (100 mL), Et_3N (12.39 g, 122.6 mmol) was added. The mixture was heated at reflux for 6 h. After evaporation, EtOAc (150 mL) was added to the residue followed by addition of H_2O (100 mL) with vigorous shaking. Organic layer was separated, dried using anhydrous Na_2SO_4, and concentrated to give the crude product, which was purified by flash column (20×4 cm, hexane/EtOAc 4:1) to afford white crystals of **11** (12.8 g, 86%); mp: 104–106 °C (Lit.[30]: 103–104 °C); ^{1}H NMR (200 MHz, [D$_6$]DMSO): δ = 11.44 (bs, 1H), 7.43–7.28 (m, 6H), 7.14 (dd, *J* = 8.2, 7.2 Hz, 1H), 6.70 (d, *J* = 8.2 Hz, 1H), 6.47 (dd, *J* = 7.6, 7.2 Hz, 1H), 6.29 (bs, 2H), 4.89 ppm (s, 2H).

Ethyl 3-benzyloxy-4-oxo-3,4-dihydroquinazolin-2-carboxylate (12): To a mixture of 2-amino-*N*-benzyloxybenzamide **11** (2 g, 8.3 mmol) in diethyl oxalate (10 mL), *para*-toluenesulfonic acid (*p*-TSA, 100 mg) was added. The mixture was held at reflux for 10 h. After cooling, the reaction mixture was passed through a silica gel column (6×3 cm) using 200 mL hexane (to remove excess diethyl oxalate) and then 200 mL EtOAc. The crude product was passed through a flash column (16×4 cm, hexane/EtOAc 4:1) to yield white crystals of **12** (1.64 g, 61%); mp: 123–124 °C; ^{1}H NMR (200 MHz, [D$_6$]DMSO): δ = 8.25 (d, *J* = 7.8 Hz, 1H), 7.93 (dd, *J* = 7.2, 7.8 Hz, 1H), 7.79 (d, *J* = 8.0 Hz, 1H), 7.68 (dd, *J* = 7.2, 7.8 Hz, 1H), 7.45 (m, 5H), 5.32 (s, 2H, CH_2), 4.41 (q, *J* = 7.0 Hz, 2H), 1.29 ppm (t, *J* = 7.0 Hz, 3H); ^{13}C NMR (50 MHz, [D$_6$]DMSO): δ = 160.0, 156.9, 145.9, 145.6, 135.6, 133.7, 130.1, 129.8, 129.1, 128.9, 128.3, 126.8, 123.8, 79.7, 63.7, 14.2 ppm; Anal. calcd for $C_{18}H_{16}N_2O_4$·0.1 hexane: C 67.10, H 5.27, N 8.41, found: C 67.41, H 4.95, N 8.75.

Ethyl 3-hydroxy-4-oxo-3,4-dihydroquinazolin-2-carboxylate (13): A solution of **12** (0.5 g, 1.54 mmol) and 10% Pd/C (50 mg) in EtOAc (10 mL) was subjected to hydrogenation for 30 min. The reaction mixture was passed through Celite, followed by evaporation and recrystallization (hexane/EtOAc) to yield pale-brown crystals of **13** (0.212 g, 59%); mp: 149–151 °C; ^{1}H NMR (200 MHz, [D$_6$]DMSO): δ = 12.43 (bs, 1H), 8.19 (d, *J* = 7.8 Hz, 1H), 7.89 (dd, *J* = 7.2, 7.4 Hz, 1H), 7.75 (d, *J* = 7.8 Hz, 1H), 7.63 (dd, *J* = 7.6, 7.2 Hz, 1H), 4.42 (q, *J* = 7.0 Hz, 2H), 1.32 ppm (t, *J* = 7.0 Hz, 3H); ^{13}C NMR (50 MHz, [D$_6$]DMSO): δ = 160.2, 157.6, 146.8, 145.9, 135.1, 128.5, 128.1, 126.6, 122.9, 63.3, 14.3 ppm; Anal. calcd for $C_{11}H_{10}N_2O_4$: C 56.41, H 4.30, N 11.96, found: C 56.37, H 4.24, N 11.97.

***N*-Benzyl-3-benzyloxy-4-oxo-3,4-dihydroquinazolin-2-carboxamide (14a)**: To a solution of **12** (0.2 g, 0.62 mmol) in EtOH (10 mL) was added benzylamine (0.33 g, 3.08 mmol). The mixture was heated at reflux for 40 h. After evaporation, the mixture was passed through a flash column (15×3 cm, hexane/EtOAc 4:1) to yield white crystals of **14a** (0.202 g, 85%); mp: 163–165 °C; ^{1}H NMR (200 MHz, [D$_6$]DMSO): δ = 9.53 (t, *J* = 5.4 Hz, 1H), 8.25 (d, *J* = 8.2 Hz, 1H), 7.93 (dd, *J* = 8.2, 7.2 Hz, 1H), 7.80 (d, *J* = 8.2 Hz, 1H), 7.70–7.62 (m, 1H), 7.42–7.27 (m, 10H), 5.31 (s, 2H), 4.51 ppm (d, *J* = 5.6 Hz, 2H); ^{13}C NMR (50 MHz, [D$_6$]DMSO): δ = 160.7, 157.2, 149.7, 146.1, 138.5, 135.5, 133.9, 130.1, 129.6, 129.0, 128.8, 128.4, 128.2, 128.0, 127.6, 126.7, 123.4, 79.8, 42.7 ppm; Anal. calcd for $C_{23}H_{19}N_3O_3$: C 71.67, H 4.97, N 10.90, found: C 71.90, H 4.94, N 10.84.

3-(Benzyloxy)-*N*-(4-fluorobenzyl)-4-oxo-3,4-dihydroquinazolin-2-carboxamide (14b): To a solution of **12** (0.3 g, 0.9 mmol) in EtOH (10 mL) was added 4-fluorobenzylamine (0.463 g, 3.7 mmol), and the reaction mixture was heated at reflux for 96 h. After evaporation, the mixture was passed through a flash column (16×3.5 cm, hexane/EtOAc 4:1). Recrystallization (EtOAc/hexane) gave white crystals of **14b** (0.323 g, 86%); mp: 192–194 °C; ^{1}H NMR (200 MHz, [D$_6$]DMSO): δ = 9.53 (bs, 1H), 8.24 (d, *J* = 7.8 Hz, 1H), 7.96–7.62 (m, 3H), 7.41–7.32 (m, 7H), 7.08–7.06 (m, 2H), 5.30 (s, 2H, CH_2), 4.49 ppm (d, *J* = 5.4 Hz, 2H); ^{13}C NMR (50 MHz, [D$_6$]DMSO): δ = 164.1, 160.7, 159.3, 157.2, 149.6, 146.0, 135.5, 134.8, 134.7, 133.9, 130.1, 129.9, 129.6, 128.9, 128.4, 128.1, 128.7, 123.4, 115.7, 115.3, 109.5, 79.7, 42.0 ppm; Anal. calcd for $C_{23}H_{18}N_3O_3$: C 68.48, H 4.50, N 10.42, found: C 68.65, H 4.47, N 10.48.

3-(Benzyloxy)-*N*-(4-chlorobenzyl)-4-oxo-3,4-dihydroquinazolin-2-carboxamide (14c): To a solution of **12** (0.3 g, 0.9 mmol) in EtOH (10 mL) was added 4-chlorobenzylamine (0.5 g, 3.7 mmol), and the reaction mixture was heated at reflux for 72 h. Upon cooling, the crystals were filtered and washed with EtOH to give white crystals of **14c** (0.265 g, 68%); mp: 203–204 °C; ^{1}H NMR (200 MHz, [D$_6$]DMSO): δ = 9.56 (t, *J* = 6.0 Hz, 1H), 8.25 (dd, *J* = 8.0, 1.0 Hz, 1H), 7.93–7.89 (m, 1H), 7.80–7.78 (m, 1H), 7.70–7.66 (m, 1H), 7.40–7.25 (m, 9H), 5.29 (s, 2H), 4.49 ppm (d, *J* = 6.0 Hz, 2H); ^{13}C NMR (50 MHz, [D$_6$]DMSO): δ = 160.7, 157.1, 149.6, 146.0, 137.6, 135.5, 133.8, 132.1, 130.1, 129.8, 129.6, 128.9, 128.7, 128.4, 128.1, 126.7, 123.4, 79.7, 42.0 ppm; Anal. calcd for $C_{23}H_{18}N_3O_3$: C 65.79, H 4.32, N 10.01, found: C 65.90, H 4.27, N 10.02.

3-(Benzyloxy)-*N*-(4-methoxybenzyl)-4-oxo-3,4-dihydroquinazolin-2-carboxamide (14d): To a solution of **12** (0.3 g, 0.9 mmol) in EtOH (10 mL) was added 4-methoxybenzylamine (0.5 g, 3.7 mmol). The reaction mixture was heated at reflux for 48 h. After evaporation, the mixture was passed through a flash column (16×3.5 cm, hexane/EtOAc 4:1). Recrystallization (EtOAc/hexane) gave white crystals of **14d** (0.288 g, 75%); mp: 162–164 °C; ^{1}H NMR (200 MHz, [D$_6$]DMSO): δ = 9.45 (t, J = 6.0 Hz, 1H), 8.24 (dd, J = 8.0, 1.0 Hz), 7.97–7.88 (m, 1H), 7.80–7.76 (m, 1H), 7.69–7.61 (m, 1H), 7.42 (s, 5H), 7.26–7.22 (m, 2H), 6.82–6.77 (m, 2H), 5.30 (s, 2H), 4.43 (d, J = 6.0 Hz, 2H), 3.71 ppm (s, 3H); ^{13}C NMR (50 MHz, [D$_6$]DMSO): δ = 160.5, 158.8, 157.1, 149.7, 146.1, 135.4, 133.9, 130.4, 130.1, 129.6, 129.4, 128.9, 128.3, 128.1, 126.7, 123.3, 114.1, 79.7, 55.5, 42.1 ppm; Anal. calcd for $C_{11}H_{10}N_2O_4$: C 69.39, H 5.10, N 10.11, found: C 69.48, H 5.08, N 10.14.

***N*-Benzyl-3-hydroxy-4-oxo-3,4-dihydroquinazolin-2-carboxamide (9a)**: To a solution of **13** (0.1 g, 0.427 mmol) in EtOH (10 mL) was added benzylamine (0.183 g, 1.708 mmol). The mixture was heated at reflux for 14 h. After evaporation, hexane (20 mL) was added to the residue, and the crystals formed were filtered. The crude product was passed through a flash column (15×3 cm, $CHCl_3$/MeOH 49:1). Recrystallization (EtOAc/hexane) gave white crystals of **9a** (81 mg, 64%). Alternatively, **9a** can be prepared as follows: to a solution of **14a** (60 mg, 0.156 mmol) in EtOAc (10 mL) was added Pd/C (10%, 15 mg) and subjected to hydrogenation for 5 h. The reaction mixture was passed through Celite. The crude product was passed through a flash column (15×2 cm, $CHCl_3$/MeOH 49:1). Recrystallization (EtOAc/hexane) gave white crystals of **9a** (11 mg, 23.9%); mp: 203–205 °C; ^{1}H NMR (200 MHz, [D$_6$]DMSO): δ = 12.29 (bs, 1H), 9.58 (t, J = 5.7 Hz, 1H), 8.16 (d, J = 7.8 Hz, 1H), 7.91–7.75 (m, 2H), 7.63–7.56 ppm (m, 1H), 7.34–7.23 (m, 5H), 4.48 (d, J = 6.2 Hz, 2H); ^{13}C NMR (50 MHz, [D$_6$]DMSO): δ = 161.4, 160.0, 147.5, 146.2, 139.2, 135.2, 128.8, 128.5, 128.2, 128.0, 127.4, 126.7, 123.2, 43.1 ppm; LRMS (ESI−) m/z (%) 278.0 (100) $[M-OH]^-$; HRMS (ESI+) calcd for $C_{16}H_{13}N_3O_3$: $[MH^+-OH]^+$ 280.1086, found: 280.1085; Analytical HPLC 99.88% purity, t_R = 5.14 min.

***N*-(4-Fluorobenzyl)-3-hydroxy-4-oxo-3,4-dihydroquinazolin-2-carboxamide (9b)**: To a solution of **13** (0.2 g, 0.854 mmol) in EtOH (10 mL) was added 4-fluorobenzylamine (0.32 g, 2.562 mmol), and the mixture was heated at reflux for 24 h. After evaporation, the mixture was passed through a flash column (15×3 cm, $CHCl_3$/MeOH 49:1) to yield white crystals of **9b** (0.143 g, 54%); mp: 217–219 °C; ^{1}H NMR (200 MHz, [D$_6$]DMSO): δ = 12.27 (bs, 1H), 9.60 (t, J = 6.2 Hz, 1H), 8.16 (d, J = 7.8 Hz, 1H), 7.92–7.75 (m, 2H), 7.64–7.56 (m, 1H), 7.43–7.35 (m, 2H), 7.20–7.08 (m, 2H), 4.45 ppm (d, J = 6.2 Hz, 2H); ^{13}C NMR (50 MHz, [D$_6$]DMSO): δ = 164.1, 161.3, 160.0, 159.3, 147.5, 146.1, 135.4, 135.3, 135.1, 130.1, 129.9, 128.5, 128.1, 126.6, 123.1, 115.6, 115.2, 42.4 ppm; LRMS (ESI−) m/z (%) 296.0 (100) $[M-OH]^-$; HRMS (ESI+) calcd for $C_{16}H_{12}FN_3O_3$: $[MH^+-OH]^+$ 298.0992, found: 298.0994; Analytical HPLC 99.84% purity, t_R = 5.04 min.

***N*-(4-Chlorobenzyl)-3-hydroxy-4-oxo-3,4-dihydroquinazolin-2-carboxamide (9c)**: To a solution of **13** (0.2 g, 0.854 mmol) in EtOH (10 mL) was added 4-chlorobenzylamine (0.363 g, 2.562 mmol), and this was heated at reflux for 24 h. After evaporation, the mixture was passed through a flash column (15×2 cm, $CHCl_3$/MeOH 49:1) to afford white crystals of **9c** (0.165 g, 59%); mp: 212–214 °C; ^{1}H NMR (200 MHz, [D$_6$]DMSO): δ = 12.29 (bs, 1H), 9.63 (t, J = 6.3 Hz, 1H), 8.16 (d, J = 7.8 Hz, 1H), 7.92–7.75 (m, 2H), 7.64–7.56 (m, 1H), 7.37 (bs, 4H), 4.46 ppm (d, J = 6.4 Hz, 2H); ^{13}C NMR (50 MHz, [D$_6$]DMSO): δ = 161.3, 160.1, 147.5, 146.1, 138.2, 135.2, 131.9, 129.8, 128.7, 128.5, 128.1, 126.6, 123.1, 42.5 ppm; LRMS (ESI−) m/z (%) 311.9 (100) $[M-OH]^-$; HRMS (ESI+) calcd for $C_{16}H_{12}ClN_3O_3$: $[MH^+-OH]^+$ 314.0696, found: 314.0693; Analytical HPLC 97.03% purity, t_R = 6.86 min.

3-Hydroxy-*N*-(4-nitrobenzyl)-4-oxo-3,4-dihydroquinazolin-2-carboxamide (9d): To a solution of **13** (0.3 g, 1.28 mmol) in EtOH (15 mL) were added 4-nitrobenzylamine hydrochloride (0.3 g, 1.54 mmol) and Et_3N (0.168 g, 1.67 mmol), and the reaction mixture was stirred at room temperature for 48 h. After evaporation, 0.1 N HCl (15 mL) was added to the residue, followed by extraction with EtOAc. Organic extract was dried by anhydrous Na_2SO_4, followed by evaporation and recrystallization (EtOAc) to yield pale-yellow crystals of **9d** (0.326 g, yield: 75%); mp: 226–228 °C; ^{1}H NMR (400 MHz, [D$_6$]DMSO): δ = 12.14 (bs, 1H), 9.59 (t, J = 6.0 Hz, 1H), 8.24 (d, J = 8.4 Hz, 2H), 8.20 (d, J = 8.0 Hz, 1H), 7.89–7.84 (m, 1H), 7.75 (d, J = 8.0 Hz, 1H), 7.66–7.59 (m, 3H), 4.62 ppm (d, J = 6.0 Hz, 2H); ^{13}C NMR (100 MHz, [D$_6$]DMSO): δ = 160.1, 157.8, 149.8, 147.1, 146.8, 146.2, 134.9, 128.7, 128.0, 127.9, 126.4, 124.0, 122.7, 42.0 ppm; Anal. calcd for $C_{16}H_{12}N_4O_5$: C 56.47, H 3.55, N 16.46, found: C 56.44, H 3.58, N 16.04.

3-Hydroxy-*N*-(4-methoxybenzyl)-4-oxo-3,4-dihydroquinazolin-2-carboxamide (9e): To a solution of **14d** (45 mg) in MeOH (5 mL) Pd/C (10%, 10 mg) was added. The mixture was subjected to hydrogenation for 20 min. The reaction mixture was passed through Celite. The crude product was passed through a flash column (15×3 cm, $CHCl_3$/MeOH 19:1) to give white crystals of **9e** (26 mg, 74%); mp: >300 °C; ^{1}H NMR (200 MHz, [D$_6$]DMSO): δ = 12.18 (t, J = 5.7 Hz, 1H), 8.03 (d, J = 8.2 Hz, 1H), 7.71–7.57 (m, 2H), 7.43–7.35 (m, 1H), 7.30 (d, J = 8.6 Hz, 2H), 6.89 (d, J = 8.6 Hz, 2H), 4.45 (d, J = 5.4 Hz, 2H), 3.72 ppm (s, 3H); ^{13}C NMR (50 MHz, [D$_6$]DMSO): δ = 162.1, 161.9, 158.7, 147.8, 144.4, 131.4, 131.3, 129.2, 128.0, 125.7, 125.1, 120.7, 114.2, 55.5, 42.3 ppm; Anal. calcd for $C_{17}H_{15}N_3O_4{\cdot}0.5\,CHCl_3$: C 54.59, H 4.06, N 10.91, found: C 54.65, H 3.74, N 10.78.

***N*-(4-Aminobenzyl)-3-hydroxy-4-oxo-3,4-dihydroquinazolin-2-carboxamide (9f)**: To a solution of **9d** (0.1 g, 0.29 mmol) in EtOH (10 mL) Pd/C (10%, 20 mg) was added. The mixture was subjected to hydrogenation for 2 h. The reaction mixture was passed through Celite. The crude product which was passed through a flash column (10×3 cm, $CHCl_3$/MeOH 49:1) to afford yellow crystals of **9f** (21 mg, 23%); mp: 243–245 °C; ^{1}H NMR (400 MHz, [D$_6$]DMSO): δ = 12.22 (bs, 1H), 9.28 (t, J = 6.2 Hz, 1H), 8.16 (d, J = 8.0 Hz, 1H), 7.89–7.85 (m, 1H), 7.76 (d, J = 8.0 Hz, 1H), 7.61–7.57 (m, 1H), 7.01 (d, J = 8.0 Hz, 2H), 6.50 (d, J = 8.4 Hz, 2H), 4.98 (s, 2H), 4.28 ppm (d, J = 6.4 Hz, 2H); LRMS (ESI−) m/z (%) 293.0 (100) $[M-OH]^-$; HRMS (ESI+) calcd for $C_{16}H_{14}N_4O_3$: $[MH^+-OH]^+$ 295.1195, found: 295.1193; Analytical HPLC 96.23% purity, t_R = 5.51 min.

***N*-(2-Chlorobenzyl)-3-hydroxy-4-oxo-3,4-dihydroquinazolin-2-carboxamide (9g)**: To a solution of **13** (0.2 g, 0.854 mmol) in EtOH (10 mL) was added 2-chlorobenzylamine (0.363 g, 2.562 mmol), and the reaction mixture was heated at reflux for 24 h. After evaporation, the mixture was passed through a flash column (15×3 cm, $CHCl_3$/MeOH 49:1) to afford white crystals of **9g** (0.155 g, 55%); mp: 191–193 °C; ^{1}H NMR (200 MHz, [D$_6$]DMSO): δ = 12.24 (bs, 1H), 9.58 (t, J = 6.0 Hz, 1H), 8.18 (d, J = 8.0 Hz, 1H), 7.93–7.77 (m, 2H), 7.65–7.57 (m, 1H), 7.47–7.27 (m, 4H), 4.56 ppm (d, J = 6.2 Hz, 2H); ^{13}C NMR (50 MHz, [D$_6$]DMSO): δ = 161.3, 160.3, 147.5, 146.0, 135.9, 135.2, 132.2, 129.5, 129.1, 129.0, 128.5, 128.1, 127.6, 126.6, 123.2, 41.2 ppm; LRMS (ESI−) m/z (%) 311.9 (100) $[M-OH]^-$; HRMS (ESI+) calcd for $C_{16}H_{12}ClN_3O_3$: $[MH^+-OH]^+$ 314.0696, found: 314.0699; Analytical HPLC 97.22% purity, t_R = 6.93 min.

***N*-(3-Chlorobenzyl)-3-hydroxy-4-oxo-3,4-dihydroquinazolin-2-carboxamide (9h)**: To a solution of **13** (0.2 g, 0.854 mmol) in EtOH

(10 mL) was added 3-chlorobenzylamine (0.24 g, 1.71 mmol), and the reaction mixture was heated at reflux for 20 h. After evaporation, the mixture was passed through a flash column (15×3 cm, $CHCl_3$/MeOH 49:1) to yield white crystals of **9h** (0.17 g, 60%); mp: 213–215 °C; ^{1}H NMR (200 MHz, [D$_6$]DMSO): δ = 12.3 (bs, 1H), 9.64 (t, J = 5.4 Hz, 1H), 8.16 (d, J = 7.6 Hz, 1H), 7.92–7.76 (m, 2H), 7.64–7.57 (m, 1H), 7.41–7.32 (m, 4H), 4.47 ppm (d, J = 6.0 Hz, 2H); ^{13}C NMR (50 MHz, [D$_6$]DMSO): δ = 161.5, 160.2, 147.3, 146.2, 141.8, 135.1, 133.4, 130.6, 128.4, 127.9, 127.8, 127.3, 126.6, 123.1, 42.7 ppm; LRMS (ESI−) *m/z* (%) 311.9 (100) $[M-OH]^-$; HRMS (ESI+) calcd for $C_{16}H_{12}ClN_3O_3$: $[MH^+-OH]^+$ 314.0696, found: 314.0705; Analytical HPLC 96.42% purity, t_R = 5.14 min.

***N*-(3,4-Dichlorobenzyl)-3-hydroxy-4-oxo-3,4-dihydroquinazolin-2-carboxamide (9i)**: To a solution of **13** (0.2 g, 0.853 mmol) in EtOH (10 mL) was added 3,4-dichlorobenzylamine (0.15 g, 0.853 mmol), and the mixture was stirred at room temperature for 48 h. After evaporation, the mixture was passed through a flash column (10× 3 cm, $CHCl_3$/MeOH 19:1) to afford white crystals of **9i** (0.183 g, 59%); mp: 226–228 °C; ^{1}H NMR (400 MHz, [D$_6$]DMSO): δ = 12.15 (bs, 1H), 9.50 (t, J = 6.0 Hz, 1H), 8.18 (d, J = 8.0 Hz, 1H), 7.89–7.85 (m, 1H), 7.74 (d, J = 8.0 Hz, 1H), 7.64–7.58 (m, 3H), 7.38–7.35 (m, 1H), 4.49 ppm (d, J = 6.0 Hz, 2H); ^{13}C NMR (100 MHz, [D$_6$]DMSO): δ = 161.0, 157.8, 149.8, 146.2, 140.0, 134.8, 131.4, 131.0, 130.0, 129.6, 128.0, 127.9, 127.8, 126.4, 122.7, 41.4 ppm; Anal. calcd for $C_{16}H_{11}Cl_2N_3O_3$: C 52.77, H 3.04, N 11.54, found: C 52.81, H 3.04, N 11.29.

3-Hydroxy-4-oxo-*N*-phenethyl-3,4-dihydroquinazolin-2-carboxamide (9j): To a solution of **13** (0.1 g, 0.426 mmol) in EtOH (10 mL) was added phenethylamine (0.155 g, 1.28 mmol), and the reaction mixture was heated at reflux for 24 h. Upon cooling, the mixture was passed through a flash column (15×3 cm, $CHCl_3$/MeOH 19:1) to afford white crystals of **9j** (0.105 g, 80%); mp: 298–300 °C; ^{1}H NMR (200 MHz, [D$_6$]DMSO): δ = 11.84 (bs, 1H), 8.04 (d, J = 8.0 Hz, 1H), 7.73–7.58 (m, 2H), 7.43–7.19 (m, 6H), 3.56–3.46 (m, 2H), 2.83 ppm (t, J = 7.6 Hz, 2H); ^{13}C NMR (50 MHz, [D$_6$]DMSO): δ = 162.1, 161.8, 147.6, 144.4, 139.8, 131.2, 129.0, 128.8, 127.9, 126.5, 125.6, 125.1, 120.7, 41.0, 35.5 ppm; Anal. calcd for $C_{17}H_{15}N_3O_3 \cdot 0.4\,CHCl_3$: C 58.53, H 4.35, N 11.91, found: C 58.90, H 4.53, N 11.89.

3-Hydroxy-4-oxo-*N*-(3-phenylpropyl)-3,4-dihydroquinazolin-2-carboxamide (9k): To a solution of **13** (0.1 g, 0.43 mmol) in EtOH (10 mL) was added 3-phenylpropan-1-amine (0.173 g, 1.28 mmol), and the reaction mixture was stirred at room temperature for 36 h. After evaporation, the mixture was passed through a flash column (15×3 cm, $CHCl_3$/MeOH 19:1) to afford white crystals of **9k** (0.116 g, 85%); mp: 108–111 °C; ^{1}H NMR (400 MHz, [D$_6$]DMSO): δ = 12.06 (bs, 1H), 8.94 (t, J = 5.6 Hz, 1H), 8.17 (d, J = 7.2 Hz, 1H), 7.88–7.84 (m, 1H), 7.74 (d, J = 8.0 Hz, 1H), 7.58 (dd, J = 6.8, 7.2 Hz, 1H), 7.31–7.16 (m, 5H), 3.18–3.24 (m, 2H), 2.66 (t, J = 7.6 Hz, 2H), 1.81 ppm (m, 2H); ^{13}C NMR (100 MHz, [D$_6$]DMSO): δ = 160.7, 157.8, 150.1, 146.2, 142.0, 134.7, 128.7, 128.6, 127.8, 127.7, 126.3, 126.2, 122.6, 38.6, 32.7, 31.0 ppm; Anal. calcd for $C_{18}H_{17}N_3O_3$: C 66.86, H 5.30, N 13.00, found: C 66.76, H 5.28, N 12.80.

Biology

Expression and purification of recombinant His-tagged NS5B polymerase

The pET expression plasmid (pET15b) encoding the His-tagged N-terminal full-length non-structural protein 5B (NS5B from HCV genotype 1b, provided by Prof. Shin Chang, Institute of Microbiology, National Taiwan University, Taiwan), and was transformed into BL21(DE3) competent cells (Yeastern Biotech, Taiwan). The bacterial cells were grown in LB plus the appropriate antibiotic at 37 °C until an OD_{600} value of 0.6 was reached. The bacterial cells were then grown at 25 °C with shaking at 300 rpm, and the expression of NS5B was initiated by the addition of glucose (0.1%) and isopropyl-β-D-thiogalactopyranoside (IPTG; 0.5 mM, Fermentas). Following incubation for 4–6 h, cells were harvested by centrifugation, and bacterial pellets were washed once with 0.5 mL ice-cold buffer A (10 mM Tris pH 8.0, 150 mM NaCl, 1 mM EDTA). The cells were resuspended in buffer A with imidazole (5 mM), NaN_3 (0.02%), DNase I (1 μg mL^{-1}), and aliquots of EDTA-free protease inhibitor cocktail tablet (Roche); they were then incubated on ice for 30 min, and the cell suspension was sonicated on ice to lyse cells (four cycles: six times for 10 s, each time with 5 s pauses in between on ice). The crude lysates were centrifuged at 13000 rpm (15000 *g*) at 4 °C for 30 min to pellet cellular debris. The lysate supernatants were then harvested and passed through a 0.22 μm filter (Millipore), and proteins >100 kDa were removed by a molecular weight cutoff membrane (Pall Life Science). The clear lysate (protein solution) was batch loaded into a nickel affinity resin (Sigma) and washed successively with a buffer containing imidazole (first 5 mM and then 25 mM) with centrifugation at 1000 rpm (140 *g*) at 4 °C for 5 min. The protein was eluted with the application of imidazole buffer (200–300 mM) with centrifugation (140 *g*) at 4 °C for 5 min. The proteins were concentrated up to 5 mg mL^{-1} by dialysis with dialysis tubing (Pierce), followed by lyophilization, and finally exchanged into buffer containing glycerol (50%), HEPES (25 mM, pH 7.5), NaCl (600 mM), and NaN_3 (0.1%) and stored at −80 °C. The protein concentration was determined with the bicinchoninic acid approach by using BCA protein assay reagent (Pierce).

HCV NS5B polymerase inhibition assay

HCV NS5B RNA-dependent RNA polymerase activity based on the generation of inorganic pyrophosphate (PPi) was performed in Luimtrac 96-well microplates (Greiner Bio-one) as follows: Reaction conditions for NS5B polymerase: HEPES (50 mM, pH 8.0), $MgCl_2$ (2.5 mM), RNAsin (20 U mL^{-1}, Promega), random heteropolymer primer (0.5 μg mL^{-1}, MDbio), RNA template isolated from HepG2 cells (5 μg mL^{-1}), NTP mixture (1 μM, Invitrogen), DTT (4 mM, Sigma), and recombinant His-tagged NS5B polymerase (1 μg mL^{-1}) in the presence or absence of compounds. The reaction mixture was supplemented with ATP sulfurylase and luciferase-coupled enzyme (each 30 μL, Cambrex Bio Science Roackland) after incubation at 37 °C for 60 min. The initiated sulfurylase-/luciferase-based reactions were incubated at 37 °C for 60 min and transferred to the Luminometer Orion II (Berthold DS, Germany) for detection of the signal generated over time at a 0.2 s reading every 30–60 s. Readings were monitored and compared with NS5B reaction without treatment as positive control (100% NS5B activity), and no NS5B reaction as negative control (0% NS5B activity means no PPi generation).

Determination of the NS5B polymerase inhibition constant and mode of inhibition

According to the PPi-based HCV NS5B RNA-dependent RNA polymerase activity assay, the reaction levels in the presence or absence of **9k** were determined by using varying concentrations of NTP (10–200 μM) with a fixed concentration of RNA template–primer as mentioned in the previous section. Inhibition data of these reactions were analyzed by Michaelis–Menten plots and double-reciprocal plots of the polymerase activity versus the con-

centration of the variable substrate for each concentration of **9k**. Data from the double-reciprocal plots were fitted to equations with linear regression for identifying V_{max} and K_M by using GraphPad Prism 4.0 software. To determine the k_{ic} and k_{iu} values, the two secondary plots were constructed according to the K_M and V_{max}, both of which were determined from the Lineweaver–Burk plot. The two inhibition constants are the intercepts of these lines with the inhibitor **9k** axis as determined by nonlinear regression (GraphPad Prism 4.0).

MTT-based cytotoxicity studies against Huh-7 and Ava.5 cells

Antiviral activity against HCV was assessed in a three-day assay using human hepatoma cell lines Ava.5 (Huh-7 cells containing sub-genomic HCV replicon, genotype 1b) and parent Huh-7 cells maintained as sub-confluent cultures on 96-well plates. The cytotoxic effects triggered by compounds were assessed for 48 h. Huh-7 and Ava.5 cells were grown at a density of 5×10^3 cells per well in 96-well plates. After 12 h, the cells were treated with compounds (0, 1, 10 μM) for an additional 48 h. Cell survival in 96-well plates was assessed by reduction. Cells were then incubated with 3-[4,5-dimethylthiazol-2-yl]-2,5-diphenyltetrazolium bromide (250 μM) at 37 °C for 3 h, and the absorbance was measured (A_{570}). Values of CC_{50} and EC_{50} are the cytotoxicities against parent Huh-7 and HCV replicon Ava.5 cells, respectively. Standard deviations for CC_{50}/EC_{50} values were calculated from standard errors generated by regression analyses. The selectivity index (SI) of compounds was calculated [$SI = CC_{50}$(Huh-7)/EC_{50}(Ava.5)] for HCV assays. Experiments were performed in quadruplicate.

Morphological examination for Huh-7 and Ava.5 cells

The morphologies of Huh-7 and Ava.5 cells after treatment with compounds were investigated by Giemsa staining. Briefly, 50000 cells were grown on glass cover slips in a six-well tissue culture plate (Corning) in FBS (10%) and antibiotic-supplemented media, and treated with compounds (50 μM each) for 48 h. The slides were then washed with distilled H_2O and stained with Giemsa solution (0.38 g Giemsa powder in 15% MeOH and 5% glycerin) followed by rinsing with distilled H_2O and differentiated with aqueous acetic acid (0.5%). Cells were dehydrated rapidly, cleared and mounted. Phase-contract micrographs were taken randomly in at least five fields of view.

Semi-quantification of HCV RNA by RT-PCR

Total cellular RNA was extracted from Ava.5 cells treated with compounds **9k** and **1** by using TRIZOL reagent (Gibco-BRL) according to the manufacturer's instructions. Quantification and purity assessment for RNA were performed by measuring optical density (OD) at λ 260 and 280 nm. Reverse transcription (RT) was carried out as follows: first 1.5 μg total RNA in 10 μL DEPC-treated H_2O containing 3 μg random hexamers was heated at 72 °C for 10 min. Then, 10 μL RT buffer containing 4 μL 5× First-Strand Buffer [250 mM Tris-HCl pH 8.3, 375 mM KCl, 15 mM $MgCl_2$, 10 pmol dNTPs, 0.2 pmol DTT, 20 U RNase inhibitor (RNase Out) and 200 U reverse transcriptase (Superscript)] were added. The final mixture was incubated at 37 °C for 1.5 h, followed by incubation at 95 °C for 5 min. All the reagents for RT were purchased from Gibco-BRL. The resultant complementary DNAs (cDNAs, 1 μg) were subsequently amplified with Taq DNA polymerase by PCR. The PCR conditions were as follows: initiation at 95 °C for 90 s, then 30 cycles at 95 °C for 30 s, 58 °C for 1 min and 72 °C for 1 min, followed by a final extension at 72 °C for 10 min. PCR reactions were performed in 50 μL reaction PCR buffer containing resultant cDNAs (1 μg), 10 pmol dNTPs, 1 U Taq DNA polymerase, 20 pmol primers, and 1.25 mM $MgCl_2$. The set of HCV primers (sense: 5′-CTG TGA GGA ACT ACT GTC TTC-3′; antisense: 5′-CAA CAC TAC TCG GCT AGC AGT-3′) were used to amplify a 221 bp region within the 5′ untranslated region (UTR) of the HCV genome. RT-PCR for glyceraldehyde 3-phosphate dehydrogenase (GAPDH) mRNA was performed in parallel to show an equal amount of total RNA in each sample. The set of GAPDH primers (sense: 5′-CCA TCA CCA TCT TCC AGG AGC G-3′; antisense: 5′-AAG GCC ATG CCA GTG AGC TTC-3′) were used to amplify a 483 bp region within GAPDH gene. All reagents for RT were purchased from Promega. The resultant cDNAs (1 μg) were subsequently used in PCR reactions to amplify the PCR products, which were visualized with UV light after resolution in a 2% agarose gel and staining with ethidium bromide.

NTP competition and displacement assays

The identification of compounds that inhibit the interaction between NTP and NS5B was carried out by using fluorescein–GTP and filtration-based competition or displacement assays. For competition assays, NS5B (5 μg mL^{-1}) and fluorescein–GTP (500 μM) were incubated at 25 °C for 30 min in the presence of various concentrations of **9k** in binding buffer (50 mM HEPES pH 8.0, 2.5 mM $MgCl_2$, 20 U mL^{-1} RNAsin, and 4 mM DTT), in a 3 kDa cutoff 96-well filtration plate. Unbound fluorescein–GTP was then removed by filtration. The fluorescence intensity of the resuspended NS5B-bound GTP was measured. For displacement assays, NS5B was first incubated with fluorescein–GTP at 25 °C for 30 min, and unbound GTP was subsequently removed by filtration. Compound **9k** was then added to the resuspended GTP–NS5B complex for an additional incubation at 25 °C for 30 min. The remaining procedures were carried out as described above. Both assays had fluorescein–GTP as positive control (100% GTP bound) and fluorescein alone as negative control (0% GTP bound).

Monitoring direct interactions of NS5B inhibitors with recombinant NS5B polymerase by QCM in the absence or presence of NTP or Mg^{2+} ions

Binding analysis of the interaction between recombinant NS5B protein and **9k** and **1** in the presence or absence of NTP and/or magnesium was performed with a quartz crystal microbalance (QCM; AffinixQμ, Initium Inc., Tokyo, Japan). Recombinant NS5B protein was absorbed directly onto the gold surface of a QCM crystal (QN sensor microsystem, Initium Inc.). First, the gold surface was cleaned by dipping in 30% H_2O_2/H_2SO_4 (1:3) for 10 min followed by rinsing thoroughly in deionized H_2O and then blowing dry under N_2 gas. This gold substrate was further used for the absorption of recombinant NS5B. NS5B proteins were spontaneously adsorbed onto the gold surface of the quartz crystal from an aqueous solution of 30 μg mL^{-1}. After 20 min, the sensor was immersed, rinsed successively with deionized H_2O and dried under N_2 gas. The immobilized NS5B generated a final signal shift of ~600 Hz, indicating that ~24 ng recombinant NS5B protein was absorbed. The NS5B immobilized quartz crystal was used for the following successive experiments. To evaluate the binding affinity of compound on NS5B, PBS (0.5 mL) with or without $MgCl_2$ (2 mM) was added, and then compound was added to the reaction chamber by the titrant injections (10, 50, 100, and/or 500 μM). The interactions were monitored by alterations in frequency (ΔF) resulting from changes in mass at the electrode surface. Validations of nonspecific binding of compounds on both control (unmodified) and reference protein

(BSA)-modified sensors were also carried out. The kinetics parameters were then determined. The same method was used to characterize the interference of **9k** on the binding of NTP and NS5B at a concentration of 200 μM. All of the binding responses were exceptionally reproducible.

Molecular modeling

The X-ray crystal structure of HCV NS5B polymerase in complex with rUTP (PDB ID: 1GX6)[31] was retrieved from the RCSB Protein Data Bank. All non-protein molecules were deleted except the two manganese ions important for catalysis. The Mn^{2+} ions were changed to Mg^{2+} ions manually and were defined as part of the receptor. The receptor was prepared by FRED Receptor 2.2.5 (OpenEye Scientific Software). The box size was adjusted to cover the two catalytic ions, the rUTP molecule, and surrounding residues with a volume size of 6832 $Å^3$. A ligand conformation library was generated by Omega 2.4.3 (OpenEye Scientific Software) with default parameters. The molecular docking simulations were performed by FRED 2.2.5 (OpenEye Scientific Software). Chemgauss3, having a metal chelation interaction term, was selected as the primary scoring function in the FRED docking parameters. The binding pose with the lowest score was selected to represent the predicted binding mode with HCV NS5B polymerase. The 3D and 2D protein–ligand interaction plots were generated by using UCSF Chimera 1.5.3 and Molecular Operating Environment, respectively.

Acknowledgements

We thank Apath LLC (St. Louis, MO, USA) for the agreement to use HCV replicon Ava.5 cells. This work was supported by National Taiwan University (99R51101).

Keywords: antiviral agents · HCV NS5B polymerase · inhibitors · pyrophosphate mimics · structure–activity relationships

[1] Q. L. Choo, G. Kuo, A. J. Weiner, L. R. Overby, D. W. Bradley, M. Houghton, *Science* **1989**, *244*, 359 – 362.
[2] U. Weiss, *Nature* **2005**, *436*, 929.
[3] J. H. Hoofnagle, *N. Engl. J. Med.* **2009**, *360*, 1899 – 1901.
[4] N. Kato, *Microb. Comp. Genomics* **2000**, *5*, 129 – 151.
[5] N. N. Zein, *Clin. Microbiol. Rev.* **2000**, *13*, 223 – 235.
[6] G. Ramadori, V. Meier, *Eur. J. Gastroenterol. Hepatol.* **2001**, *13*, 465 – 471.
[7] Q. M. Wang, B. A. Heinz, *Prog. Drug Res.* **2000**, *55*, 1 – 32.
[8] M. P. Manns, J. G. McHutchison, S. C. Gordon, V. K. Rustgi, M. Shiffman, R. Reindollar, Z. D. Goodman, K. Koury, M. Ling, J. K. Albrecht, *Lancet* **2001**, *358*, 958 – 965.
[9] M. W. Fried, M. L. Shiffman, K. R. Reddy, C. Smith, G. Marinos, F. L. Goncales, Jr., D. Haussinger, M. Diago, G. Carosi, D. Dhumeaux, A. Craxi, A. Lin, J. Hoffman, J. Yu, *N. Engl. J. Med.* **2002**, *347*, 975 – 982.
[10] J. J. Feld, J. H. Hoofnagle, *Nature* **2005**, *436*, 967 – 972.
[11] P. L. Beaulieu, Y. S. Tsantrizos, *Curr. Opin. Investig. Drugs* **2004**, *5*, 838 – 850.
[12] C. A. Lesburg, M. B. Cable, E. Ferrari, Z. Hong, A. F. Mannarino, P. C. Weber, *Nat. Struct. Biol.* **1999**, *6*, 937 – 943.
[13] R. R. Deore, J.-W. Chern, *Curr. Med. Chem.* **2010**, *17*, 3806 – 3826.
[14] National Library of Medicine, Specialized Information Services, The US National Institutes of Health: http://clinicaltrials.gov (accessed September 24, **2011**).
[15] J. Quer, M. Buti, M. Cubero, J. Guardia, R. Esteban, J. I. Esteban, *Infect. Drug Resist.* **2010**, *3*, 133 – 145.
[16] S. E. Behrens, L. Tomei, R. De Francesco, *EMBO J.* **1996**, *15*, 12 – 22.
[17] I. Bougie, S. Charpentier, M. Bisaillon, *J. Biol. Chem.* **2003**, *278*, 3868 – 3875.
[18] V. Summa, A. Petrocchi, P. Pace, V. G. Matassa, R. De Francesco, S. Altamura, L. Tomei, U. Koch, P. Neuner, *J. Med. Chem.* **2004**, *47*, 14 – 17.
[19] P. Pace, E. Nizi, B. Pacini, S. Pesci, V. Matassa, R. De Francesco, S. Altamura, V. Summa, *Bioorg. Med. Chem. Lett.* **2004**, *14*, 3257 – 3261.
[20] I. Stansfield, S. Avolio, S. Colarusso, N. Gennari, F. Narjes, B. Pacini, S. Ponzi, S. Harper, *Bioorg. Med. Chem. Lett.* **2004**, *14*, 5085 – 5088.
[21] S. Yan, T. Appleby, E. Gunic, J. H. Shim, T. Tasu, H. Kim, F. Rong, H. Chen, R. Hamatake, J. Z. Wu, Z. Hong, Y. Yao, *Bioorg. Med. Chem. Lett.* **2007**, *17*, 28 – 33.
[22] V. Summa, A. Petrocchi, F. Bonelli, B. Crescenzi, M. Donghi, M. Ferrara, F. Fiore, C. Gardelli, O. G. Paz, D. J. Hazuda, P. Jones, O. Kinzel, R. Laufer, E. Monteagudo, E. Muraglia, E. Nizi, F. Orvieto, P. Pace, G. Pescatore, R. Scarpelli, K. Stillmock, M. V. Witmer, M. Rowley, *J. Med. Chem.* **2008**, *51*, 5843 – 5855.
[23] E. D. Jones, N. Vandegraff, G. Le, N. Choi, W. Issa, K. Macfarlane, N. Thienthong, L. J. Winfield, J. A. V. Coates, L. Lu, X. Li, X. Feng, C. Yu, D. I. Rhodes, J. J. Deadman, *Bioorg. Med. Chem. Lett.* **2010**, *20*, 5913 – 5917.
[24] C.-S. Chen, C.-T. Chiou, G. S. Chen, S.-C. Chen, C.-Y. Hu, W.-K. Chi, Y.-D. Chu, L.-H. Hwang, P.-J. Chen, D.-S. Chen, S.-H. Liaw, J.-W. Chern, *J. Med. Chem.* **2009**, *52*, 2716 – 2723.
[25] R. R. Deore, G. S. Chen, C.-S. Chen, P.-T. Chang, M.-H. Chuang, T.-R. Chern, H.-C. Wang, J.-W. Chern, *Curr. Med. Chem.* **2012**, *19*, 613 – 624.
[26] A. Agrawal, C. A. F. de Oliveira, Y. Cheng, J. A. Jacobsen, J. A. McCammon, S. M. Cohen, *J. Med. Chem.* **2009**, *52*, 1063 – 1074.
[27] F. C. Lahser, B. A. Malcolm, *Anal. Biochem.* **2004**, *325*, 247 – 254.
[28] U. Koch, B. Attenni, S. Malancona, S. Colarusso, I. Conte, M. Di Filippo, S. Harper, B. Pacini, C. Giomini, S. Thomas, I. Incitti, L. Tomei, R. De Francesco, S. Altamura, V. G. Matassa, F. Narjes, *J. Med. Chem.* **2006**, *49*, 1693 – 1705.
[29] M. Billamboz, F. Bailly, M. L. Barreca, L. D. Luca, J. F. Mouscadet, C. Calmels, M. L. Andeola, M. Witvrouw, F. Christ, Z. Debyser, P. Cotelle, *J. Med. Chem.* **2008**, *51*, 7717 – 7730.
[30] M. D. Surman, M. J. Mulvihill, M. J. Miller, *Org. Lett.* **2002**, *4*, 139 – 141.
[31] S. Bressanelli, L. Tomei, F. A. Rey, R. De Francesco, *J. Virol.* **2002**, *76*, 3482 – 3492.

Received: January 30, 2012
Published online on March 1, 2012

